Mineralocorticoid receptor knockout in Schwann cells alters myelin sheath thickness

Alberto González-Mayoral, Axel Eid, Razmig Derounian, Virginia Sofia Campanella, Andreia da Silva Ramos, Romy El Khoury, Charbel Massaad, Damien Le Menuet

Mineralocorticoid Receptor knockout in Schwann cells alters myelin sheath thickness

Alberto González-Mayoral[1,2], Axel Eid[1,3], Razmig Derounian[1], Virginia Sofia Campanella[1], Andreia da Silva Ramos[1], Romy El Khoury[1], Charbel Massaad[1], Damien Le Menuet[1]*

1.INSERM UMRS 1124 (T3S), Faculty of Basic and Biomedical Sciences, *Université Paris Cité*, Paris, France.

2. Current address: Paris Brain Institue-*Institut du Cerveau*, CNRS UMR7225, INSERM U1127, *Hôpital de la Pitié Salpétrière*, Paris, France

3. Current address: INSERM UMR 1195 (DHNS), Faculty of Medicine, *Université Paris-Saclay*, Le Kremlin-Bicêtre, France.

* Corresponding author:

Damien Le Menuet, PhD

INSERM T3S (UMRS_1124)

Myelination and Nervous System Pathologies

45 rue des Saints Pères

75006 Paris

France

Tel +33 1 76 53 43 82

Email: damien.le-menuet@inserm.fr

https://orcid.org/0000-0002-0802-7190

Short title: MR, a new player in Schwann Cells

Keywords: Peripheral Nervous System, Schwann Cells, Glucocorticoids, Mineralocorticoid Receptor

Abstract

Myelination allows fast and synchronized nerve influxes and is provided by Schwann cells in the peripheral nervous system. Glucocorticoid hormones are major regulators of stress, metabolism and immunity affecting all tissues. They act by binding to two receptors, the low affinity glucocorticoid receptor (GR) and the high affinity mineralocorticoid receptor (MR). Little is known on the effect of glucocorticoid hormones on the PNS and this study focuses on deciphering the role of MR in peripheral myelination. In this work, the presence of a functional MR in Schwann cells is demonstrated and the expression of MR protein in mouse sciatic nerve SC is evidenced. Besides, knockout of MR in SC (SCMRKO using Cre-lox system with *DesertHedgeHog* (Dhh) Cre promoter) was undertaken in mice. SCMRKO was not associated with alterations of performance in motor behavioral tests on 2- to 6-month old male mice compared to their controls. No obvious modifications of myelin gene expression or MR signaling gene expression were observed in the SCMRKO sciatic nerves. Nevertheless, *Gr* transcript and GR protein amounts were significantly increased in SCMRKO nerves compared to controls, suggesting a possible compensatory effect. Besides, an increase in myelin sheath thickness was noted for axons with perimeters larger than 15 µm in SCMRKO illustrated by a significant 4.5 % reduction in g-ratio (axon perimeter/myelin sheath perimeter). Thus, we defined MR as a new player in peripheral system myelination and in SC homeostasis.

Introduction

Myelin sheaths allow rapid and coordinated nerve influx in vertebrates. In the peripheral nervous system (PNS), myelination is insured by Schwann cells (SC) (Boullerne 2016), each SC myelinating a unique axon. Alternatively, small caliber axons of less than 1 µm in diameter and with low conduction velocities are grouped together by non-myelinating SC (Salzer 2012). Myelin lesions occur in several pathologies including auto-immune diseases such as Guillain–Barré syndrome (Shahrizaila *et al.* 2021), genetic diseases such as Charcot-Marie-Tooth often caused by mutations in myelin-associated genes (Higuchi & Takashima 2022), and diabetic neuropathy (Naruse 2019). Additionally, a repair process involving demyelination followed by remyelination is involved in wound healing after nerve injury (Ding & Hammarlund 2019). Many factors regulate the differentiation and function of Schwann cells such as several hormonal signaling mediated by members of the nuclear receptor superfamily (Mangelsdorf *et al.* 1995). For instance, thyroid hormones (Barakat-Walter & Kraftsik 2018), androgens (Magnaghi *et al.* 2001), progesterone (Schumacher *et al.* 2012) and estrogens (Gu *et al.* 2018) have been reported to improve peripheral nerve regeneration. Glucocorticoid hormones (GC) are also able to promote remyelination and nerve regeneration after injury (Hughes 2002; Morisaki *et al.* 2010; Feng & Yuan 2015) although it is not clear if their effects are due to their anti-inflammatory properties or to their endogenous action on SC homeostasis. Conversely, some adverse effects have been reported with antenatal and perinatal GC exposure (Damsted *et al.* 2011) such as on the myelination of the auditory nerve in preterm sheep (Rittenschober-Böhm *et al.* 2018). Glucocorticoid actions are mediated by two highly homologous members of the nuclear receptor superfamily, the mineralocorticoid receptor MR, coded by the *Nr3c2* gene also named *Mr* (Viengchareun *et al.* 2007) and the glucocorticoid receptor GR (Oakley & Cidlowski 2013) coded by *Nr3c1* gene, also named *Gr*. Both receptor mRNA were previously reported to be expressed in rodent sciatic nerves and in SC-derived cell lines (Groyer *et al.* 2006; Girard *et al.* 2010). MR presents a high affinity for glucocorticoids and is also able to bind specifically the mineralocorticoid hormone aldosterone. As aldosterone plasmatic

concentration is 100 times lower than that of glucocorticoids, some mechanisms of hormonal specificity occur in mineralocorticoid-sensitive tissues, mainly in the sodium transporting tight epithelia. In these tissues, aldosterone is mostly known to regulate ion homeostasis (Pearce *et al.* 2022). A mechanism of mineralocorticoid selectivity is the action of the enzyme 11βHSD2 in tight epithelia that metabolized active glucocorticoids into inactive compounds (Farman & Bocchi 2000). In other MR-expressing tissues such as heart, blood vessels, smooth muscles, nervous system, 11βHSD2 expression is absent or very low indicating that, at least in a non-pathological situation, MR should probably be considered as a high affinity receptor for GC (Le Menuet & Lombès 2014). However, it was reported that in some experimental conditions, the prerequisites for aldosterone signaling, such as 11βHSD2 expression are present in SC (Groyer *et al.* 2006; Girard *et al.* 2010). GR affinity for GC is around 10 times lower than that of MR. It has been proposed that GR and MR act in balance depending of the concentration of GC which follows circadian variations with a peak after waking and a trough at the beginning of the sleeping period. Altogether, this indicates that concerning glucocorticoid actions, it is important to consider the contributions of both MR and GR receptors. A low concentration of GC such as during the trough of the circadian rhythm is considered to be already sufficient to occupy most of MR receptors while binding to GR is significant only at the daily peak of GC concentration and under stress (de Kloet *et al.* 2005).

Because of the major importance of GC hormones regulating stress, circadian rhythm, metabolism, immunity and in affecting all the tissues (Kadmiel & Cidlowski 2013), it is of great value to investigate GC actions in the PNS that have been little studied so far (Madalena & Lerch 2017). We focused here on the role of MR in the PNS. We revealed the expression and functionality of MR in SC in vitro and in vivo and developed a mouse model of SC specific MR knockout, SCMRKO. GR expression in the sciatic nerve was increased in SCMRKO mice indicating a possible compensation by GR after MR loss. No motor behavioral abnormalities were evidenced in this model, however, myelin sheaths of axons larger than 15 µm in perimeter were enlarged in the sciatic nerves.

Materials and Methods

Cell culture. MSC80 (Baron-Van Evercooren *et al.* 1992) cells (a gift form *Institut du Cerveau* (ICM), Inserm U1127, Paris France) were cultured as previously described (Shackleford *et al.* 2018). For hormonal treatment and antagonists, cells were plated at 50,000 cells/ wells of 12 well plates and changed in serum-free medium after two days. Treatment was performed the following day. Aldosterone, spironolactone, dexamethasone and RU486 (all from Roche) were diluted in ethanol, and added at 1/10,000 final dilution each in culture medium. Primary SC cultures derived from E13.5 mouse dorsal root ganglia (pregnant C57BL/6 dams from Janvier Labs, Le Genest-Saint-Isle, France) that were dissociated in trypsin, plated and grown as previously described (Sundaram *et al.* 2021). Confluent cultures were used to seed 12 well plates at 50,000 cells/wells and treatments were performed as described with MSC80 cells. The proliferation and differentiation medium were free of serum.

Reverse Transcription-quantitative PCR. RNA from cells and sciatic nerves, the latter homogenized with a bead mill (Fisherbrand, Illkirch, France), were extracted with Trizol reagent (Life Technologies). Reverse Transcriptions were performed with one µg of total RNA (unless stated otherwise)**.** After DNAse treatment (Promega), RNA were reverse-transcribed with MMLV reverse transcriptase (Thermofisher) in a 50 µL volume according to the manufacturer instructions. qPCR were performed with 0.7 µL of RT using Sybr Green (Thermofisher) reagent. The primer sequences are listed in Table 1. RT are amplified with a CFX384 Touch Real-Time PCR Detection System (Biorad). Results are the mean of experimental triplicates and were analyzed according to the ΔΔCT method. For each set of experiments, the normalization gene was determined as the one showing the lowest variations from a series of 10 normalization genes (Sundaram *et al.* 2019).

Animals and behavioral tests. MR fl/fl animals were generated by Berger et al. (Berger *et al.* 2006), and were kindly provided by Dr Frédéric Jaisser, Inserm U1138, *Centre de Recherche des Cordeliers*, Paris, France. Jackson Laboratory provided the dhhCre animals (FVB(Cg)-Tg(Dhh-cre)1Mejr/J, strain 112929), both lines being previously backcrossed in the C57BL/6J

genetic background. This project received the agreement number C750607 and was approved by the animal facility (*Plateforme d'hébergement et d'élevage*, BiomedTech facilities, *Université Paris Cité*), the local ethic comity (Ceea40) and received the number D750607 by the French government. Animals were housed with a 12 h light/dark cycle under constant temperature. Behavioral tests were performed between 10 and 12 AM with groups of littermate males. Four to five mice of both genotypes were reared in the same cage. Animals were tested each month between 2 and 6-month of ages. For the grip strength test (Bioseb, Vitrolles, France), animals were tested on two different days of the same week each month. The highest value of three trials for the forepaws and three trials for the four limbs was recorded. Eventually the averages of the two monthly values were calculated. For rotarod (Orchid Scientific, Dehli, India), mice were also tested at two different days. For each day, each animal was tested twice with interval of at least 30 minutes between passages, and the mean values were recorded (time and distance walked). For automatic locomotor test Locotronic® (Intellibio, Seichamps, France), animals crossed the ladder 3 times, with a 30-minute lag. Two sessions each month were averaged. The values (number of errors, and travel times) of the first trial were ignored, being considered as habituation.

Genomic PCR. Tissues were lysed at 55°C overnight in buffer containing NaCl 200 mM, SDS 5 mM, EDTA 5 mM, Tris 100 mM (pH 8.5), 0.5 mg/ mL proteinase K then spin at 12,000 g. Supernatant were precipitated with isopropanol, spin at 12,000 g, then DNA was solubilized in water. PCR reactions were performed according to the conditions previously described for MR flox allele (Berger *et al.* 2006) and from Jackson laboratories for dhhCre allele. Primers are listed in Table 1.

Immunofluorescence. Four-month old mouse sciatic nerves were dissected and fixed in paraformaldehyde 4% in PBS at 4°C overnight., incubated in 10 mM citrate ph=6 at 95°C 5 minutes for antigen retrieval. Nerves were then incubated in sucrose 20% in OCT (optimal cutting temperature, Thermofisher) in a mold and froze. Twelve µm thick sections were cut with a cryostat and disposed on 3-(triethoxysily)propylamine (TESPA)-treated slides. Section

were then permeabilized with 0.2% triton X100, 0.1% tween 20, blocked with 2% BSA and 5% donkey serum in PBS tween 0.1%, incubated at 4°C overnight with primary antibodies (rabbit anti-MR Thermofisher PA-95019, 1/100 and goat anti-sox10 R&D AF 2864 1/200 as previously validated (Sundaram *et al.* 2021)) then incubated with secondary antibodies (donkey anti-rabbit Alexa 488 1/2,000 and donkey anti-goat Cy3 1/500, Jackson IR). Nuclei were labeled with Hoescht, slides were mounted in coverslips with fluoromount-G (Thermofisher) and dry overnight. Slides were observed with an Axio Observer inverted microscope (Zeiss). Images were snapped with Zen 3.2 software (Zeiss) and elaborated using the same parameters for each sample. For immunocytochemistry, cells were grown in 8 chamber slides (labTek, Thermo Fisher) in the same conditions described in the cell culture chapter. Cells were then fixed in paraformaldehyde 4% for 15 min, wash and permeabilized for 5 min in 0.2% Triton X100, 0.1% Tween 20, blocked in 5% BSA and Lab-Teks then treated similarly to the nerve sections. GR monoclonal rabbit antibody (D6H2L, Cell Signaling) was used at 1/200 (Delangre *et al.* 2021) .

Western blot.

Sciatic nerves were homogenized with a bead mill (FisherBrand) in RIPA buffer containing protease inhibitors (Roche). Thirty µg of protein were loaded and migrated in SDS PAGE 10% acrylamide/bis-acrylamide. Gels were transferred on nitrocellulose membranes and incubated overnight (4°C) with primary antibodies (rabbit anti-MR Thermofisher PA-95019, 1/250 or rabbit anti-GR Cell signaling D6H2L 1/1,000 (Chen *et al.* 2019) and mouse anti-αtubulin Sigma-Aldrich T6074 1/10,000), then with secondary antibodies (goat anti-rabbit IgG Dylight 800 and anti-mouse IgG Dylight 680 at 1:10,000 each, from Thermo Scientific) 1 h at room temperature. An Odyssey infrared imaging system (LI-COR, Bad Homburg, Germany) was used to scan membranes. Bands were quantified with Odyssey Application Software version 3.0 (Li-COR).

Transmission electron microscopy and g-ratio determination. Sciatic nerves were fixed in paraformaldehyde 4% glutaraldehyde 25% solution, then stained with osmium tetroxide and embedded in epoxy resin as previously described (Makoukji *et al.* 2011). Ultrathin 50 nm sections were performed and visualized by Transmission Electron Microscope JEOL 1011 in the PIME core facility (*Institut Cochin*, Paris, France). g-ratio was calculated using Image J software dividing the inside perimeter of the myelin sheath by the outside perimeter. Around 150 to 200 sheaths by nerve were quantified and the captions were spread over the total surface of the nerve section.

Statistical analysis. Statistical analyses were conducted using Mann-Whitney test, suitable for non-parametric comparisons of two experimental groups. The g-ratio statistical analyses were performed with student t-test, adapted to compare two groups of values presenting a gaussian distribution.

Results

Functional MR and GR signaling in Schwann Cells in vitro

The MSC80 cell line was spontaneously immortalized from mouse sciatic nerve (Baron-Van Evercooren *et al.* 1992) and retained the expression of several myelinating SC-specific markers such as MPZ, PMP22 and Krox20 (Shackleford *et al.* 2018). Expression of MR and GR protein was detected by immunocytochemistry together with the SC specific transcription factor Sox10 (Fig 1A), as well as in Western blot (Fig 1B). Expression of the glucocorticoid target gene *Per1* transactivated by both MR and GR (Le Billan *et al.* 2015) was then used as an index of both receptors functionality in MSC80. Cells were treated for 3 hours in a serum free medium by aldosterone (Aldo), the physiological specific MR ligand, dexamethasone (Dex), a synthetic glucocorticoid that binds only to GR, spironolactone an MR antagonist, RU486 a GR antagonist, then *Per1* expression was measured by RT-qPCR. Both agonists were able to significantly stimulate *Per1* at different levels (Aldo 2-fold stimulation; Dex 8-fold stimulation) expression while antagonists specifically repressed the agonistic effect (Fig 1C). Treatments with each antagonist (Spiro, RU) did not modify *Per1* expression. This indicates that MR and GR are functional in the MSC80 cell line. A time-course experiment under aldosterone treatment showed that Per1 expression was stimulated after a 2 h treatment and stimulation persisted for 24 h; this timeline being compatible with a transcriptional effect of MR (Fig. 1D). MR and GR expressions were detected in primary Schwann cell cultures (pSC) derived from E13.5 mouse dorsal root ganglia with immunofluorescence, colocalizing with Sox10 (Fig. 1E). This preparation method allows to obtain a very pure SC culture with low fibroblast contaminations compared to SC cultures isolated from sciatic nerve (Sundaram *et al.* 2021). Indeed, only few cells are negative for Sox10 as visualized in the merged panel (Fig. 1E). The receptor expression levels were then investigated in pSC. Cultures can be maintained either in proliferation or on differentiation phenotype after cAMP treatment. Both *Mr* and *Gr* transcripts were clearly detected (Fig. 1F and 1G) by RT-qPCR, in proliferative and differentiating pSC cultures and the *Mr* expression level appeared to be 10 to 15 times lower

than *Gr*, as observed in many tissues (Farman & Bocchi 2000). The qPCR cycle threshold (CT) numbers (Fig. 1H) are indicated to evaluate the scale of the expression level for each gene. The functionality of the receptors in differentiated pSC cultures was assessed measuring the expression of the MR and GR target gene *Fkbp5* (Le Billan *et al.* 2015) under agonists and antagonists treatment. As with MSC80 cells, in primary culture, MR and GR were able to transactivate a target gene in presence of the agonists while the antagonists abolished this effect (Fig. 1G). The lower transactivation potency of MR compared to GR may be due in part to its lower expression level. Altogether, these data show that both glucocorticoid receptors MR and GR are expressed and respond to their ligands in SC-derived cellular models and pSC.

Generation of a mouse knockout model for MR in Schwann cells

To better understand MR's role in the peripheral nervous system, MR knockout targeted in SC was performed by breeding the MR flox/flox (MR fl/fl) mice, and the dhhCre mouse line harboring the SC-specific promoter of Desert hedgehog driving the expression of the Cre recombinase cDNA (Zhang *et al.* 2019). Both models were characterized and validated in previous studies (Berger *et al.* 2006; Wu *et al.* 2008; Rickard *et al.* 2012). After two generations, MR fl/fl animals (Control, Ctrl) were crossed to MR fl/fl dhhCre/+ mice (with *Mr* knockout in SC, SCMRKO) and were stably bred (Fig 2A). Sex ratio and genotype repartition were as expected in the breeding, and SCMRKO were viable and healthy. Nerve specific excision of MR in SCMRKO animals was visualized by PCR. For negative controls to test the specificity of the excision DNA from hippocampus (Hip) were used, where myelination is ensured by oligodendrocytes and does not contain SC, as well as liver lobes (LV) which are poorly innervated and highly vascularized (Fig. 2B). Brachial nerve (Nv) DNA was used to visualize the excision. Figure 2B shows PCR products from a control (Ctrl) and an SCMRKO mouse using primers from dhhCre (290 bp) transgene and for the MR fl construct (345 bp) or the excised allele (390 bp) for the 3 sets of DNA (Nv, Hip, Lv). In SCMRKO animals, excision of

the MR fl construct is only visible in the brachial nerve DNA. Only the flox allele amplification is found in hippocampus, and liver DNA, the latter indicating no excision in blood vessels and endothelial cells. The expression of *Mr* in sciatic nerves was then assessed by qPCR in Ctrl and SCMRKO mice (Fig. 2C). A significant 50% reduction in MR expression was observed in SCMRKO animals. A total suppression of *Mr* expression and total *Mr* excision in SCMRKO was not expected as sciatic nerves also contain blood vessels composed of smooth muscle cells as well as fibroblasts which express MR (Pruthi *et al.* 2014). As female sex hormones are reported to present an effect on myelination (Schumacher *et al.* 2012; Gu *et al.* 2018) and are secreted cyclically, at this stage only males have been explored.

In situ validation of Schwann Cell MR knockout in the sciatic nerve

In order to validate in situ the specificity of MR knockout in SC, immunofluorescence was performed to analyze the co-localization of MR with the SC-specific transcription factor Sox10 in sciatic nerve. The labeling obtained in sciatic nerve from 6-month-old Ctrl and SCMRKO mice are shown, respectively (Figs. 3A and B). The negative control incubating the slices with solely secondary antibodies did not show any labeling (Fig. 3C). Zooming (white rectangles) in Ctrl nerve (Fig. 3D) and SCMRKO nerve (Fig. 3E), showed that, despite some background noise in MR labeling especially inside the axons, a clear colocalization of MR with Sox10 is observed in the nuclei of sciatic nerve from Ctrl animals (Fig. 3D, merged panel) while no labeling above background noise is observed for Sox10 positive cells in SCMRKO animals, albeit few cells show some weak, background-like, MR-antibody staining (see grey arrow). To our knowledge, this is the first visualization of MR protein expression in SCs reported to date. Indeed, previous studies in sciatic nerves have detected Mr RNA or indirectly aldosterone binding by MR (Groyer *et al.* 2006). These data validate the specificity of SC MR knockout confirming genomic PCR data (Fig. 2B).

Functional assessment of MR knockout in Schwann Cells

First, we showed that there was no difference in body weight between Ctrl and SCMRKO animals (Fig. 4A). Several motor behavioral tests were performed with male Ctrl and SCMRKO mice every month from 2 to 6 months of age. In the rotarod test mice are put on an accelerating rotating rod inducing a force motor activity. The time preceding the fall off the rod of the animal is measured (Fig. 4B) and there was no significant effect of the inactivation of MR in SC. Grip strength test allows to measure the maximum strength of a mouse either with its forepaws griping a rod, either with its four limbs griping a grid. There was no difference between control and SCMRKO mice for the strength measured with forepaws alone, which revealed also the ability to grasp (Fig. 4C) as well as with the four limbs (Fig. 4D). Motor coordination while walking was tested with the automatic locomotor test (Locotronic®) consisting in the monitoring of the crossing of a horizontal ladder. Neither the number of errors (stumbling between rungs, Fig. 4E) nor the travel time was modified in SCMRKO animals (Fig. 4F). Only the results at 6 months are presented as in younger ages the number of errors was low.

MR knockout is associated with GR upregulation in sciatic nerves

To further analyze the effect of MR knockout in SC, the expression levels of several SC specific genes were measured in Ctrl and SCMRKO sciatic nerves from 3-month old male mice by qPCR (Fig. 5). *Krox20* (or *Egr2*) encodes for a transcription factor specific of myelinating SC while *p75NTR* encodes for the receptor for neurotrophins that characterized the non-myelinating SC. There were no significant differences between groups for the mRNA expression of this genes (Fig. 5A and 5B). mRNA expressions of *Mpz*, *Pmp22* and *Mbp* genes, all coding for structural proteins of the myelin sheath were also not significantly modified in SCMRKO (Fig. 5C, D and E). Besides, there is no clear trend on MPZ protein quantity compared between groups (Fig. 5F) apart for a larger variability among individuals for SCMRKO sciatic nerves. Concerning glucocorticoid signaling genes in the sciatic nerve, MR

and GR target genes *Sgk* (Fig. 6A) and *Per1* (Fig. 6B) transcript expressions are not significantly modified by the knockout of *Mr* in SC while a significant 35% increase of *Gr* mRNA expression was measured in SCMRKO (Fig. 6C). The protein level of MR and GR in SCMRKO mouse sciatic nerve were examined by Western blot (Fig.6 D and E). As found for *Mr* transcripts, MR quantity is decreased by around 30% in SCMRKO ($p<0.05$) compared to controls, reflecting *Mr* excision in the SC (Fig. 6D). Concerning GR, a significant 50% increase ($p<0.05$; of note around 35% increase, without outlier point in SCMRKO nerve, $p=0.0258$, not shown) of GR protein amount was measured in SCMRKO sciatic nerve lysates, consistent with the results obtained with *Gr* transcripts (Fig. 6E). As *Mr* knockout in SC is associated with an increase GR protein amount in the sciatic nerve, it would be difficult to separate the effects of MR from that of GR with this animal model.

MR inactivation is associated with larger myelin sheaths around large caliber axons

Subsequently, morphological examination of transversal sciatic nerve section was performed with transmission electron microscopy. Sections were from both nerves of six animals that underwent the locomotor tests (Fig. 7A and B) at 6 months of age. Myelin (M) sheaths formed dark layers around axons. In some places the presence of SC cellular bodies and nuclei are visible. Remak Bundles (RB) are composed of unmyelinated SC surrounding several small caliber axons corresponding to sensitive fibers. Thickness of the myelin sheath compared to the diameter of the axon was assessed by calculating the g-ratio, which corresponds to the inner perimeter of the myelin sheath divided by its outer perimeter, therefore g-ratio is always less than 1. Determining the g-ratio value showed that it is significantly smaller (0.699) in SCMRKO animals, thus corresponding to larger myelin sheaths compared to control (0.713; $p<0.0001$, Fig. 7C). To have a better understanding of this difference, g-ratio distribution was examined as a function of the values of axon perimeters (Fig. 7D). There was no difference between groups for axon smaller than 15 µm in perimeter. Besides, a significant decrease of g-ratio, corresponding to myelin sheath enlargement, was found in SCMRKO axons between

15 to 25 µm of axon perimeter (15 to 20 µm: Ctrl g-ratio=0.724 vs 0.690 for SCMRKO, $p<0.0001$; 20 to 25 µm, Ctrl g-ratio=0.740 vs 0.708 for SCMRKO, $p<0.001$, >25µm Ctrl g-ratio=0.775 vs 0.745 for SCMRKO; $p<0.01$ with student t-test). As a whole, for axon perimeters larger than 15 µm, g-ratios decrease by around 4.5% in SCMRKO animals. Scatter plot of g-ratio values further revealed the lower g-ratio for the SCMRKO sheaths associated with a less marked regression curve slope (Fig. 5E). Apart for sheath thickness, there were no obvious morphological differences between the two groups.

Discussion.

The study of glucocorticoid hormone actions, putting aside their anti-inflammatory properties, is a blind spot in the scientific literature on the peripheral nervous system, especially concerning Schwann cells (Groyer *et al.* 2006; Girard *et al.* 2010). Considering the crucial importance of glucocorticoid hormones in regulating the functions of most tissues in mammals, the investigation of their role in the PNS is of great interest. We demonstrated here that both receptors, MR and GR are expressed and functional in Schwann cells. We then focused on the function of MR because it is a high affinity receptor for glucocorticoids. The specific deletion of *Mr* gene in mouse Schwann cells is associated with an increase of myelin sheath thickness for large caliber axons but with no modification of locomotor behavior at 6 months of age. It is noteworthy that, for the sake of reducing the number of animals used, the same group of mice has performed all tests at different ages and animals with no training may have performed differently in some tests after the age of two months. Additionally, some differences may have emerged after 6 months of age. An issue not addressed in this work was the potential effect of *Mr* deletion in unmyelinating SC that interact with low diameter axons of sensitive fibers, forming the Remak bundles. However no major motor behavior alterations were noted in SCMRKO animals, as expected in the case of alterations of sensitive fiber functions that can

cause neuropathic pain (Gross & Üçeyler 2020). This indicates that a major role of MR in unmyelinating SC is not likely to be revealed by this model.

Importantly, *Mr* excision is also associated with an increase of *Gr* transcripts and GR protein amounts in the sciatic nerve. This raises the question whether the modification of myelin thickness observed in SCMRKO sciatic nerves is due to the absence of MR in Schwann cells or to the overabundance of GR. It is also possible that the increase of GR quantity is a compensatory mechanism masking some consequences of MR absence. Interestingly, increase of GR quantity after MR excision was previously reported with the knockout of MR in the mouse hippocampus (Oakley *et al.* 2021). All this hints to the fact that MR and GR actions are combinatorial in SC.

In the first decades following MR characterization, it was thought that its expression was restricted to the sodium transporting tight epithelia, the hippocampus in the CNS and the cardiovascular system, while GR expression was described as being ubiquitous (Funder 1996). Although sometimes hard to put in evidence due to a lower expression level compared to GR and some technical difficulties in immunodetection, it appears now that MR expression could be widespread. Indeed, MR physiological importance is now well established in, for instance, skin (Sevilla & Pérez 2018), white (Infante *et al.* 2019) and brown (Kuhn *et al.* 2018) adipocytes as well as in eye tissues (Canonica *et al.* 2021). Recently several studies focused also on the analysis of the role of MR in skeletal muscle (Hauck *et al.* 2019; Hulse *et al.* 2022). Along this line, a locomotor MR and GR axis encompassing motor neuron (Kretz *et al.* 2001), Schwann cell and skeletal muscle that remains to be characterized may be hypothesized. Of note, the clinical relevance of MR in skeletal muscle is illustrated by the development of new therapeutic strategies involving the use of MR antagonists to treat Duchenne muscular dystrophy (Howard *et al.* 2022).

Because MR excision in Schwann cells resulted in an increase of GR abundance, the role of MR in peripheral myelination may not be understood without analyzing in parallel the role of GR. Interestingly, MR and GR target gene *Sgk1* total knockout in mouse resulted in a

decreased g-ratio of the same magnitude than in SCMRKO animals, and suggested that SGK1 regulates myelination by phosphorylating NDRG1 (Heller *et al.* 2014). Moreover, it has been recently proposed that SGK may be a molecular switch for glial regeneration after injury in the PNS (Okura *et al.* 2022). This further highlight a potential involvement of glucocorticoid signaling in peripheral myelination.

In some tissues, MR overactivation seems to be associated with pathological states linked with inflammation such as in the cardiovascular and immune systems. The knockout of MR specifically in cardiomyocytes (Rickard *et al.* 2012), myeloid cells (Li *et al.* 2014), macrophages (Bienvenu *et al.* 2012), vascular smooth muscle cells (Pruthi *et al.* 2014) and endothelial cells (Jia *et al.* 2015) result in a better resistance to experimentally induced injury. Eventually, that may be also tested in the SCMRKO model using, for instance, sciatic nerve crush experiments. Along this line, MR antagonists are now widely used in medicine for the treatment of cardiovascular system pathologies and is currently under development for other pathologies (Epstein 2015). That raises the question of the exact role of MR in normal physiology in these organs, and how to reveal it in term of protocol in animal experimentation. For instance, it may be considered that rodents in animal facilities are very well fed, poorly exercised and kept in thermal neutrality. These conditions may not be optimal to reveal the potential benefits of MR signaling. On the other hand, non-pathological actions of MR are better understood principally in aldosterone-sensitive sodium transporting epithelia (Epstein *et al.* 2022) and in limbic system neurons (Joëls & de Kloet 2017). For the latter, it is now clear that study of MR and GR actions cannot be dissociated (Oakley *et al.* 2021).

In conclusion, glucocorticoid hormones present widespread actions in vertebrates and their roles in the peripheral nervous system are not well understood, most particularly the contribution of their receptors MR and GR. It is important to gain more insights in this field of research as glucocorticoid compounds are among the most prescribed drugs (Martins & de Castro 2021) and glucocorticoid hormones are key mediators in stress, immunity and

411 metabolism (Oakley & Cidlowski 2013) whose dysregulations are damaging for the peripheral
412 nervous system and are central in pathologies induced by modern lifestyle.

413

414

Acknowledgements

We are indebted to Dr. Frédéric Jaisser; Inserm U1138, *Centre de Recherche des Cordeliers* to provide the MR fl/fl mice originally obtained by Berger et al (Berger *et al.* 2006). We thank UMS BioMedTech facilities, *Campus Saint Germain des Près*, *Université Paris Cité*, for providing access to the molecular and cellular biology platform Cyto2BM, and also for the housing and breeding of the mice. We are particularly indebted with Claire Mader, head of the animal facility, for helping to set up the project authorization request and Isis Blanchard for her expertise with the locomotor test devices. We are grateful to the electron microscopy platform, *Université Paris Cité*, *Institut Cochin* and to its director Alain Schmitt for the nerve ultrathin sections and their imaging. We thank Dr. Venkat Krishan Sundaram for providing the RT reactions used in Fig. 1F and 1G, and Céline Dargenet-Becker for the primary Schwann cell culture used for immunofluorescence in Fig 1E.

Fundings

This work was support with recurrent funding from INSERM and *Université Paris Cité*. AGM was recipient from a fellowship from the *Fundación Universidad de Burgos*, under the *Viveuropa* European Union program and *Castilla y León* Regional Government, Spain.

Author Contributions

DLM and CM designed the study. DLM wrote the first draft of the manuscript, performed the experiments, and calculated the g-ratio on TEM images. AGM contributed to the writing of the manuscript, the preparation of electron microscopy samples with VSC and together with AE, performed the behavioral test, qPCR experiments, Western blot experiments and set up the immunofluorescence conditions. RD, VSC, AdSR, REK realized qPCR experiments, Western blot immunocytochemistry and further help to the setting up of the immunofluorescence

experiments. All authors read and amended the manuscript as well as agreed with its final content.

Declaration of interest: None

References

Barakat-Walter I & Kraftsik R 2018 Stimulating effect of thyroid hormones in peripheral nerve regeneration: research history and future direction toward clinical therapy. Neural Regeneration Research 13 599–608. (https://doi.org/10.4103/1673-5374.230274)

Baron-Van Evercooren A, Gansmuller A, Duhamel E, Pascal F & Gumpel M 1992 Repair of a myelin lesion by Schwann cells transplanted in the adult mouse spinal cord. Journal of Neuroimmunology 40 235–242. (https://doi.org/10.1016/0165-5728(92)90139-c)

Berger S, Wolfer DP, Selbach O, Alter H, Erdmann G, Reichardt HM, Chepkova AN, Welzl H, Haas HL, Lipp H-P & Schütz G 2006 Loss of the limbic mineralocorticoid receptor impairs behavioral plasticity. Proceedings of the National Academy of Sciences of the United States of America 103 195–200. (https://doi.org/10.1073/pnas.0503878102)

Bienvenu LA, Morgan J, Rickard AJ, Tesch GH, Cranston GA, Fletcher EK, Delbridge LMD & Young MJ 2012 Macrophage mineralocorticoid receptor signaling plays a key role in aldosterone-independent cardiac fibrosis. Endocrinology 153 3416–3425. (https://doi.org/10.1210/en.2011-2098)

Boullerne AI 2016 The history of myelin. Experimental Neurology 283 431–445. (https://doi.org/10.1016/j.expneurol.2016.06.005)

Canonica J, Zhao M, Favez T, Gelizé E, Jonet L, Kowalczuk L, Guegan J, Le Menuet D, Viengchareun S, Lombès M, Pussard E, Arsenijevic Y & Behar-Cohen F 2021 Pathogenic Effects of Mineralocorticoid Pathway Activation in Retinal Pigment Epithelium. International Journal of Molecular Sciences 22 9618. (https://doi.org/10.3390/ijms22179618)

Chen H, Amazit L, Lombès M & Le Menuet D 2019 Crosstalk Between Glucocorticoid Receptor and Early-growth Response Protein 1 Accounts for Repression of Brain-derived Neurotrophic Factor Transcript 4 Expression. Neuroscience 399 12–27. (https://doi.org/10.1016/j.neuroscience.2018.12.012)

Damsted SK, Born AP, Paulson OB & Uldall P 2011 Exogenous glucocorticoids and adverse cerebral effects in children. European Journal of Paediatric Neurology: EJPN: Official Journal of the European Paediatric Neurology Society 15 465–477. (https://doi.org/10.1016/j.ejpn.2011.05.002)

Delangre E, Liu J, Tolu S, Maouche K, Armanet M, Cattan P, Pommier G, Bailbé D & Movassat J 2021 Underlying mechanisms of glucocorticoid-induced β-cell death and dysfunction: a new role for glycogen synthase kinase 3. Cell Death & Disease 12 1136. (https://doi.org/10.1038/s41419-021-04419-8)

Ding C & Hammarlund M 2019 Mechanisms of injury-induced axon degeneration. Current Opinion in Neurobiology 57 171–178. (https://doi.org/10.1016/j.conb.2019.03.006)

Epstein M 2015 Reduction of cardiovascular risk in chronic kidney disease by mineralocorticoid receptor antagonism. The Lancet. Diabetes & Endocrinology 3 993–1003. (https://doi.org/10.1016/S2213-8587(15)00289-2)

Epstein M, Kovesdy CP, Clase CM, Sood MM & Pecoits-Filho R 2022 Aldosterone, Mineralocorticoid Receptor Activation, and CKD: A Review of Evolving Treatment Paradigms. American Journal of Kidney Diseases: The Official Journal of the National Kidney Foundation S0272-6386(22)00744-2. (https://doi.org/10.1053/j.ajkd.2022.04.016)

Farman N & Bocchi B 2000 Mineralocorticoid selectivity: molecular and cellular aspects. Kidney International 57 1364–1369. (https://doi.org/10.1046/j.1523-1755.2000.00976.x)

Feng X & Yuan W 2015 Dexamethasone enhanced functional recovery after sciatic nerve crush injury in rats. BioMed Research International 2015 627923. (https://doi.org/10.1155/2015/627923)

Funder JW 1996 Mineralocorticoid receptors and glucocorticoid receptors. Clinical Endocrinology 45 651–656. (https://doi.org/10.1046/j.1365-2265.1996.8540862.x)

Girard C, Eychenne B, Schweizer-Groyer G & Cadepond F 2010 Mineralocorticoid and glucocorticoid receptors in sciatic nerve function and regeneration. The Journal of Steroid Biochemistry and Molecular Biology 122 149–158. (https://doi.org/10.1016/j.jsbmb.2010.07.005)

Gross F & Üçeyler N 2020 Mechanisms of small nerve fiber pathology. Neuroscience Letters 737 135316. (https://doi.org/10.1016/j.neulet.2020.135316)

Groyer G, Eychenne B, Girard C, Rajkowski K, Schumacher M & Cadepond F 2006 Expression and functional state of the corticosteroid receptors and 11 beta-hydroxysteroid dehydrogenase type 2 in Schwann cells. Endocrinology 147 4339–4350. (https://doi.org/10.1210/en.2005-1625)

Gu Y, Wu Y, Su W, Xing L, Shen Y, He X, Li L, Yuan Y, Tang X & Chen G 2018 17β-Estradiol Enhances Schwann Cell Differentiation via the ERβ-ERK1/2 Signaling Pathway and Promotes Remyelination in Injured Sciatic Nerves. Frontiers in Pharmacology 9 1026. (https://doi.org/10.3389/fphar.2018.01026)

Hauck JS, Howard ZM, Lowe J, Rastogi N, Pico MG, Swager SA, Petrosino JM, Gomez-Sanchez CE, Gomez-Sanchez EP, Accornero F & Rafael-Fortney JA 2019 Mineralocorticoid Receptor Signaling Contributes to Normal Muscle Repair After Acute Injury. Frontiers in Physiology 10 1324. (https://doi.org/10.3389/fphys.2019.01324)

Heller BA, Ghidinelli M, Voelkl J, Einheber S, Smith R, Grund E, Morahan G, Chandler D, Kalaydjieva L, Giancotti F, King RH, Fejes-Toth AN, Fejes-Toth G, Feltri ML, Lang F & Salzer JL. 2014 Functionally distinct PI 3-kinase pathways regulate myelination in the peripheral nervous system. The Journal of Cell Biology 204 1219–1236. (https://doi.org/10.1083/jcb.201307057)

Higuchi Y & Takashima H 2022 Clinical genetics of Charcot-Marie-Tooth disease. Journal of Human Genetics. (https://doi.org/10.1038/s10038-022-01031-2)

Howard ZM, Gomatam CK, Piepho AB & Rafael-Fortney JA 2022 Mineralocorticoid Receptor Signaling in the Inflammatory Skeletal Muscle Microenvironments of Muscular Dystrophy and Acute Injury. Frontiers in Pharmacology 13 942660. (https://doi.org/10.3389/fphar.2022.942660)

Hughes R a. C 2002 Systematic reviews of treatment for inflammatory demyelinating neuropathy. Journal of Anatomy 200 331–339. (https://doi.org/10.1046/j.1469-7580.2002.00041.x)

Hulse JL, Habibi J, Igbekele AE, Zhang B, Li J, Whaley-Connell A, Sowers JR & Jia G 2022 Mineralocorticoid receptors mediates diet - induced lipid infiltration of skeletal muscle and insulin resistance. Endocrinology bqac145. (https://doi.org/10.1210/endocr/bqac145)

Infante M, Armani A, Marzolla V, Fabbri A & Caprio M 2019 Adipocyte Mineralocorticoid Receptor. Vitamins and Hormones 109 189–209. (https://doi.org/10.1016/bs.vh.2018.10.005)

Jia G, Habibi J, DeMarco VG, Martinez-Lemus LA, Ma L, Whaley-Connell AT, Aroor AR, Domeier TL, Zhu Y, Meininger GA, Mueller KB, Jaffe IZ & Sowers JR 2015 Endothelial Mineralocorticoid Receptor Deletion Prevents Diet-Induced Cardiac Diastolic Dysfunction in Females. Hypertension (Dallas, Tex.: 1979) 66 1159–1167. (https://doi.org/10.1161/HYPERTENSIONAHA.115.06015)

Joëls M & de Kloet ER 2017 30 YEARS OF THE MINERALOCORTICOID RECEPTOR: The brain mineralocorticoid receptor: a saga in three episodes. The Journal of Endocrinology 234 T49–T66. (https://doi.org/10.1530/JOE-16-0660)

Kadmiel M & Cidlowski JA 2013 Glucocorticoid receptor signaling in health and disease. Trends in Pharmacological Sciences 34 518–530. (https://doi.org/10.1016/j.tips.2013.07.003)

de Kloet ER, Joëls M & Holsboer F 2005 Stress and the brain: from adaptation to disease. Nature Reviews. Neuroscience 6 463–475. (https://doi.org/10.1038/nrn1683)

Kretz O, Schmid W, Berger S & Gass P 2001 The mineralocorticoid receptor expression in the mouse CNS is conserved during development. Neuroreport 12 1133–1137. (https://doi.org/10.1097/00001756-200105080-00017)

Kuhn E, Lamribet K, Viengchareun S, Le Menuet D, Fève B & Lombès M 2018 UCP1 transrepression in Brown Fat in vivo and mineralocorticoid receptor anti-thermogenic effects. Annales d'Endocrinologie. (https://doi.org/10.1016/j.ando.2018.04.018)

Le Billan F, Khan JA, Lamribet K, Viengchareun S, Bouligand J, Fagart J & Lombès M 2015 Cistrome of the aldosterone-activated mineralocorticoid receptor in human renal cells. FASEB Journal: Official Publication of the Federation of American Societies for Experimental Biology 29 3977–3989. (https://doi.org/10.1096/fj.15-274266)

Le Menuet D & Lombès M 2014 The neuronal mineralocorticoid receptor: from cell survival to neurogenesis. Steroids 91 11–19. (https://doi.org/10.1016/j.steroids.2014.05.018)

Li C, Zhang YY, Frieler RA, Zheng XJ, Zhang WC, Sun XN, Yang QZ, Ma SM, Huang B, Berger S, Wang W, Wu Y, Yu Y, Duan SZ & Mortensen RM 2014 Myeloid mineralocorticoid receptor deficiency inhibits aortic constriction-induced cardiac hypertrophy in mice. PloS One 9 e110950. (https://doi.org/10.1371/journal.pone.0110950)

Madalena KM & Lerch JK 2017 The Effect of Glucocorticoid and Glucocorticoid Receptor Interactions on Brain, Spinal Cord, and Glial Cell Plasticity. Neural Plasticity 2017 8640970. (https://doi.org/10.1155/2017/8640970)

Magnaghi V, Cavarretta I, Galbiati M, Martini L & Melcangi RC 2001 Neuroactive steroids and peripheral myelin proteins. Brain Research. Brain Research Reviews 37 360–371. (https://doi.org/10.1016/s0165-0173(01)00140-0)

Makoukji J, Shackleford G, Meffre D, Grenier J, Liere P, Lobaccaro J-MA, Schumacher M & Massaad C 2011 Interplay between LXR and Wnt/β-catenin signaling in the negative regulation of peripheral myelin genes by oxysterols. The Journal of Neuroscience: The Official Journal of

570 the Society for Neuroscience 31 9620–9629. (https://doi.org/10.1523/JNEUROSCI.0761-
571 11.2011)

572 Mangelsdorf DJ, Thummel C, Beato M, Herrlich P, Schütz G, Umesono K, Blumberg B, Kastner
573 P, Mark M, Chambon P & Evans RM 1995 The nuclear receptor superfamily: the second
574 decade. Cell 83 835–839. (https://doi.org/10.1016/0092-8674(95)90199-x)

575 Martins CS & de Castro M 2021 Generalized and tissue specific glucocorticoid resistance.
576 Molecular and Cellular Endocrinology 530 111277.
577 (https://doi.org/10.1016/j.mce.2021.111277)

578 Morisaki S, Nishi M, Fujiwara H, Oda R, Kawata M & Kubo T 2010 Endogenous glucocorticoids
579 improve myelination via Schwann cells after peripheral nerve injury: An in vivo study using a
580 crush injury model. Glia 58 954–963. (https://doi.org/10.1002/glia.20977)

581 Naruse K 2019 Schwann Cells as Crucial Players in Diabetic Neuropathy. Advances in
582 Experimental Medicine and Biology 1190 345–356. (https://doi.org/10.1007/978-981-32-9636-
583 7_22)

584 Oakley RH & Cidlowski JA 2013 The biology of the glucocorticoid receptor: new signaling
585 mechanisms in health and disease. The Journal of Allergy and Clinical Immunology 132 1033–
586 1044. (https://doi.org/10.1016/j.jaci.2013.09.007)

587 Oakley RH, Whirledge SD, Petrillo MG, Riddick NV, Xu X, Moy SS & Cidlowski JA 2021
588 Combinatorial actions of glucocorticoid and mineralocorticoid stress hormone receptors are
589 required for preventing neurodegeneration of the mouse hippocampus. Neurobiology of Stress
590 15 100369. (https://doi.org/10.1016/j.ynstr.2021.100369)

591 Okura A, Inoue K, Sakuma E, Takase H, Ueki T & Mase M 2022 SGK1 in Schwann cells is a
592 potential molecular switch involved in axonal and glial regeneration during peripheral nerve
593 injury. Biochemical and Biophysical Research Communications 607 158–165.
594 (https://doi.org/10.1016/j.bbrc.2022.03.123)

595 Pearce D, Manis AD, Nesterov V & Korbmacher C 2022 Regulation of distal tubule sodium
596 transport: mechanisms and roles in homeostasis and pathophysiology. Pflugers Archiv:
597 European Journal of Physiology 474 869–884. (https://doi.org/10.1007/s00424-022-02732-5)

598 Pruthi D, McCurley A, Aronovitz M, Galayda C, Karumanchi SA & Jaffe IZ 2014 Aldosterone
599 promotes vascular remodeling by direct effects on smooth muscle cell mineralocorticoid
600 receptors. Arteriosclerosis, Thrombosis, and Vascular Biology 34 355–364.
601 (https://doi.org/10.1161/ATVBAHA.113.302854)

602 Rickard AJ, Morgan J, Bienvenu LA, Fletcher EK, Cranston GA, Shen JZ, Reichelt ME,
603 Delbridge LM & Young MJ 2012 Cardiomyocyte mineralocorticoid receptors are essential for
604 deoxycorticosterone/salt-mediated inflammation and cardiac fibrosis. Hypertension (Dallas,
605 Tex.: 1979) 60 1443–1450. (https://doi.org/10.1161/HYPERTENSIONAHA.112.203158)

606 Rittenschober-Böhm J, Rodger J, Jobe AH, Kallapur SG, Doherty DA, Kramer BW, Payne MS,
607 Archer M, Rittenschober C, Newnham JP, Miura Y, Berger A, Matthews SG & Kemp MW 2018
608 Antenatal Corticosteroid Exposure Disrupts Myelination in the Auditory Nerve of Preterm
609 Sheep. Neonatology 114 62–68. (https://doi.org/10.1159/000487914)

610 Salzer JL 2012 Axonal regulation of Schwann cell ensheathment and myelination. Journal of
611 the Peripheral Nervous System: JPNS 17 Suppl 3 14–19. (https://doi.org/j.1529-
612 8027.2012.00425.x)

613 Schumacher M, Hussain R, Gago N, Oudinet J-P, Mattern C & Ghoumari AM 2012
614 Progesterone synthesis in the nervous system: implications for myelination and myelin repair.
615 Frontiers in Neuroscience 6 10. (https://doi.org/fnins.2012.00010)

616 Sevilla LM & Pérez P 2018 Roles of the Glucocorticoid and Mineralocorticoid Receptors in
617 Skin Pathophysiology. International Journal of Molecular Sciences 19 E1906.
618 (https://doi.org/ijms19071906)

Shackleford G, Sampathkumar NK, Hichor M, Weill L, Meffre D, Juricek L, Laurendeau I, Chevallier A, Ortonne N, Larousserie F, Herbin M, Bièche I, Coumoul X, Beraneck M, Baulieu EE, Charbonnier F, Pasmant E & Massaad C. 2018 Involvement of Aryl hydrocarbon receptor in myelination and in human nerve sheath tumorigenesis. Proceedings of the National Academy of Sciences of the United States of America 115 E1319–E1328. (https://doi.org/10.1073/pnas.1715999115)

Shahrizaila N, Lehmann HC & Kuwabara S 2021 Guillain-Barré syndrome. Lancet (London, England) 397 1214–1228. (https://doi.org/10.1016/S0140-6736(21)00517-1)

Sundaram VK, Sampathkumar NK, Massaad C & Grenier J 2019 Optimal use of statistical methods to validate reference gene stability in longitudinal studies. PloS One 14 e0219440. (https://doi.org/10.1371/journal.pone.0219440)

Sundaram VK, El Jalkh T, Barakat R, Fernandez CJI, Massaad C & Grenier J 2021 Retracing Schwann Cell Developmental Transitions in Embryonic Dissociated DRG/Schwann Cell Cocultures in Mice. Frontiers in Cellular Neuroscience 15 590537. (https://doi.org/10.3389/fncel.2021.590537)

Viengchareun S, Le Menuet D, Martinerie L, Munier M, Pascual-Le Tallec L & Lombès M 2007 The mineralocorticoid receptor: insights into its molecular and (patho)physiological biology. Nuclear Receptor Signaling 5 e012. (https://doi.org/10.1621/nrs.05012)

Wu J, Williams JP, Rizvi TA, Kordich JJ, Witte D, Meijer D, Stemmer-Rachamimov AO, Cancelas JA & Ratner N 2008 Plexiform and dermal neurofibromas and pigmentation are caused by Nf1 loss in desert hedgehog-expressing cells. Cancer Cell 13 105–116. (https://doi.org/10.1016/j.ccr.2007.12.027)

Zhang S-J, Li X-X, Yu Y, Chiu AP, Lo LH, To JC, Rowlands DK & Keng VW 2019 Schwann cell-specific PTEN and EGFR dysfunctions affect neuromuscular junction development by impairing Agrin signaling and autophagy. Biochemical and Biophysical Research Communications 515 50–56. (https://doi.org/10.1016/j.bbrc.2019.05.014)

645

Figure legends

Figure 1. MR and GR are expressed and functional in primary Schwann cell cultures. A) Immunocytochemistry on MR (green), Sox10 (red) and GR (green) in MSC80 cells. MR and Sox10 pictures are in the same field. Ctrl-, negative control: merged field with Hoescht (blue) and secondary antibodies only; white bar is 10 µm. B) MR and GR proteins are detected by western blot in lysates from Schwann cell derived MSC80 cells (untreated cells in duplicate). C) Hormonal treatment of MSC80 cells; VEH, vehicle (ethanol); Aldo, aldosterone 10^{-8} M; Aldo Spiro: Aldosterone 10^{-8} M and Spironaloctone 10^{-6} M; DEX: dexamethasone 10^{-7} M; DEX RU: dexamethasone 10^{-7} M and RU486 (mifepristone) 10^{-6} M; Spiro: Spironolactone 10^{-6} M; and RU: RU486 10^{-6} M. *Per1* expression was measured by RT-qPCR using ΔΔCT with *Mrlp10* normalization gene (n=6 wells/treatment). Statistical analysis, Mann Whitney test; ** vs Veh $p<0.01$; # vs Aldo $p<0.05$; $$ vs DEX $p<0.01$. D) MSC80 were treated with Veh and Aldo for 2 hours (2h), 3 hours (3h) and 24 hours (24h), and Per1 expression was analyzed by the ΔΔCT method using *Mrlp10* normalization gene (n=6 wells/condition). Mann Whitney test; ** $p<0.01$ vs VEH 2h; $$ $p<0.01$ vs VEH 3h and ## $p<0.05$ vs VEH 24 hours. E) Immunocytochemistry on GR (green), Sox10 (red) and MR (green) in Primary SC cultures. MR and Sox10 and merged are from the same field; white bar 10µm. White star (*), MR positive Sox10 negative cell. Ctrl-, negative control: merged field with Hoescht (blue) and secondary antibodies only; white bar is 10 µm F, G, H) Analysis of MR and GR signaling in primary Schwann cell cultures (pSC, bright field mid-center) from mouse E13.5 embryo dorsal root ganglia. *Mr* and *Gr* mRNA expression are assessed in Proliferative (Prol) and Differentiating (Dif) pSC. H) MR and GR qPCR determined CT (from 500 ng RNA RT) are reported from 2 individual cultures in Prol or Dif culture conditions. F) and G) qPCR amplification of *Mr* and *Gr*, respectively, on the same samples normalized by ΔΔCT method with *Sdha* and *Mrpl10* gene expression (n=3 wells/treatment for ech graphs). *Mr* expression level is around one tenth of *Gr* expression. G) Expression of MR and GR target gene *Fkbp5* in differentiating primary Schwann cell culture measure by RT-qPCR and normalized by ΔΔCT method with *Hsp60* expression (N=6

673 wells/treatment). VEH, vehicle (ethanol); Aldo, aldosterone 10^{-8} M; Aldo Spiro, aldosterone 10^{-8} M + Spironolactone 10^{-6} M; DEX, dexamethasone 10^{-7} M; DEX RU, dexamethasone 10^{-7} M + RU486 10^{-6} M. Mann Whitney test; **, p<0.01 vs Veh; ##, p<0001 vs Aldo; $$, p<0.01 vs DEX; error bars +/- SD

677 **Figure 2**. **Generation of SCMRKO mice.** MRSCKO mice were generated by crossing the MR flox/flox (MR fl/fl) mouse strain with the dhhCre strain, generating heterozygous animals (MR flox/+) that are subsequently backcrossed to obtain MR fl/fl and MR fl/fl/ dhhCre animals to fund the breeding colony (Fig 2A). Illustrations are from BioRender free version. B) Gel electrophoresis of PCR products amplified on genomic DNA from brachial nerve (Nv), hippocampus (Hip), Liver (Lv) for dhhCre transgene of a SCMRKO mouse and a control (Ctrl) mouse. Left gel; MW, molecular weight; dhhCre transgene amplification, transgene 290 bp (base pairs), control d9mit sequence 148 bp (Ctrl Allele). Right gel, MR flox construct amplification; flox allele, 345 bp, excised allele 390 bp; white star (*) excision of the flox allele in brachial nerve. See Table1 for primer sequences. For the flox allele, MR fl Rv2 primer (table I) is too distant from MR fl Fw primer for amplification while for the excised allele, MR fl Rv1 primer is deleted and MR fl Rv2 is closer to the forward primer and able to amplify the 390 bp fragment. C) Expression of *Mr* in control (Ctrl, N=13) and SCMRKO (N=11) 3-month old male sciatic nerve measured by RT-qPCR using the ΔΔCT method normalizing with *Rpl13a* gene expression; means +/- SEM; Mann Whithney test, ** p<0.01 vs Ctrl; error bars +/- SD.

692

693 **Figure 3. Validation of SCMRKO by immunofluorescence.** Cryosections (12 µm) of sciatic nerves from 6-month old control MR flox/flox (MRfl/fl, A) and SCMRKO (B) animals were labeled with anti-MR antibody (green) or anti Sox 10 antibody (red) and nucleus were stained with Hoechst (blue), scale: 50 µm. Control secondary antibodies only (Neg Ctrl) was stained and the same conditions (C). White rectangles in A and B indicate zooming areas. Magnifications of a representative field are shown in D (Control, Ctrl) and E (SCMRKO) with each channel presented separately with a 10 µm scale; Hoechst (blue), MR labeling (green)

Sox10 labeling (red) and a merged channel (lower right panel). White arrows indicate Sox10 positive Schwann cell nuclei, co-labeled for MR in Ctrl and with no MR labeling in SCMRKO. The grey arrow indicates a Sox10 positive cell, background-like, weakly positive cell for MR (E).

Figure 4. **Phenotypic characterization of the motor function of SCMRKO mice.** A) Animals were weight at 2, 5 and 6 months. MRfl/fl control animals are noted C, KO: SCMRKO animals. No significant differences (Mann Whitney test). B) Rotarod test was performed on the same animals, time before fall of the animal (y axis) was measured each month on two to six month old male mice. Experiments stopped after 300 s. C are control mice (N=11), KO for SCMRKO animal (N=12). No difference between groups (Mann Whitney test).Grip strength test (y axis force in grams), with the forelimb only (C) and with four limbs (D), same animals, same notations than in A) and B). No significant difference between groups (Mann Whitney test, comparison of the data for each group every month). Locotronic test, number of errors (E) and travel time (F) are reported in y axis at 6 months (Mann Whitney test), same animals; Ctrl: MRfl/fl mice; no significant differences; error bars +/- SD.

Figure 5. Consequences of SCMRKO on sciatic nerve gene and protein expression. Expression of SC genes *Krox20* (A), *p75* (B), *Pmp22* (C), *Mpz* (D), and *Mbp* (E) were assessed by RT-qPCR from 3-month old mouse sciatic nerve RNA of control (Ctrl, N=14) and SCMRKO (N=11). Expression was measured with the $\Delta\Delta$CT method normalizing with *Rpl13a* gene expression. Results are expressed as fold change compared to Ctrl sciatic nerve expression which was set to 1. Statistical analysis by Mann Whitney test indicated that differences between the two groups were not significant. F) Upper panel, 4-month old mice Control (Ctrl N=9) or SCMRKO (N=9) were blotted and revealed with anti-MPZ antibody and αTubulin

(αTub) antibody for normalization. Lower panel, quantification with mean of the control set to 1; Mann Whitney test, not significant; error bars +/- SD.

Figure 6. SCMRKO effect on MR signaling pathway in sciatic nerve. The expression of mineralocorticoid signaling genes *Per1* (A) , *Sgk* (B) and *Gr* (C) was measured by qPCR. Differences between group were not significant with Mann Whitney test except for *Gr* expression, (* p<0.05, vs Ctrl). D). Upper panel, sciatic nerve lysates from 3 to 4 month old male mice. Control (Ctrl N=14) or SCMRKO (N=14) were blotted and revealed with anti-MR antibody and anti-αTubulin (αTub) antibody for normalization. Lower panel, signals were quantified and mean of the control was set to 1; * p<0.05 vs Ctrl, Mann Whitney test. E) Upper panel, 4-month old mice Control (Ctrl N=15) or SCMRKO (N=15) were blotted and revealed with anti-GR antibody and αTubulin (αTub) antibody for normalization. Lower panel, quantification with mean of the control set to 1; * p<0.05 vs Ctrl Mann Whitney test; error bars +/- SD.

Figure 7. Decreased g-ratio in SCMRKO sciatic nerve myelin sheath. Transmission electron microscopy imaging of control (Ctrl, A) and SCMRKO (B) sciatic nerve cross section. SC, Schwann cell cytoplasm and nuclei; RB, Remak Bundle; Ax, Axon; M, Myelin sheath. C) g-ratios of myelin sheaths from left and right sciatic nerves of 6 month old mice (N=3 animals for each group) were determined with image J and plotted individually from control (Ctrl, circles, mean=0.713) and SCMRKO (squares; mean=0.713); t test; **** p<0.0001 vs Ctrl. D) g-ratios were then plotted according to the distribution of axon perimeter, from <10 µm to > 25 µm with 5 µm perimeter categories; Control (Ctrl), SCMRKO (KO); t test; NS, non-significant; **** p<0.0001 vs Ctrl, ### p<0.001 vs Ctrl. E) With the same data from C, g-ratios were represented in a scatter plot as a function of the axon perimeter for control (Ctrl) and SCMRKO myelin sheaths, with representation of the linear regression; error bars +/- SD.

Table 1. Primer sequences. For each primer pairs, Fw: forward primers, Rv: Reverse primers. D9mit is a control sequence for the genotyping of dhhCre transgene; MR fl, MR flox allele primers from Berger et al (Berger *et al.* 2006). *Hsp60* (*Heat Shock Protein Family D Member 1*), *Mrlp10* (*Mitochondrial Ribosomal Protein L10*), *Sdha (Succinate Dehydrogenase Complex Subunit A*) and *Rpl13a* (*Ribosomal Protein L13a*) are normalization genes whose use is indicating accordingly in the corresponding legends. Each of these normalization genes has been selected using the method described in Sundaram et al (Sundaram *et al.* 2019).

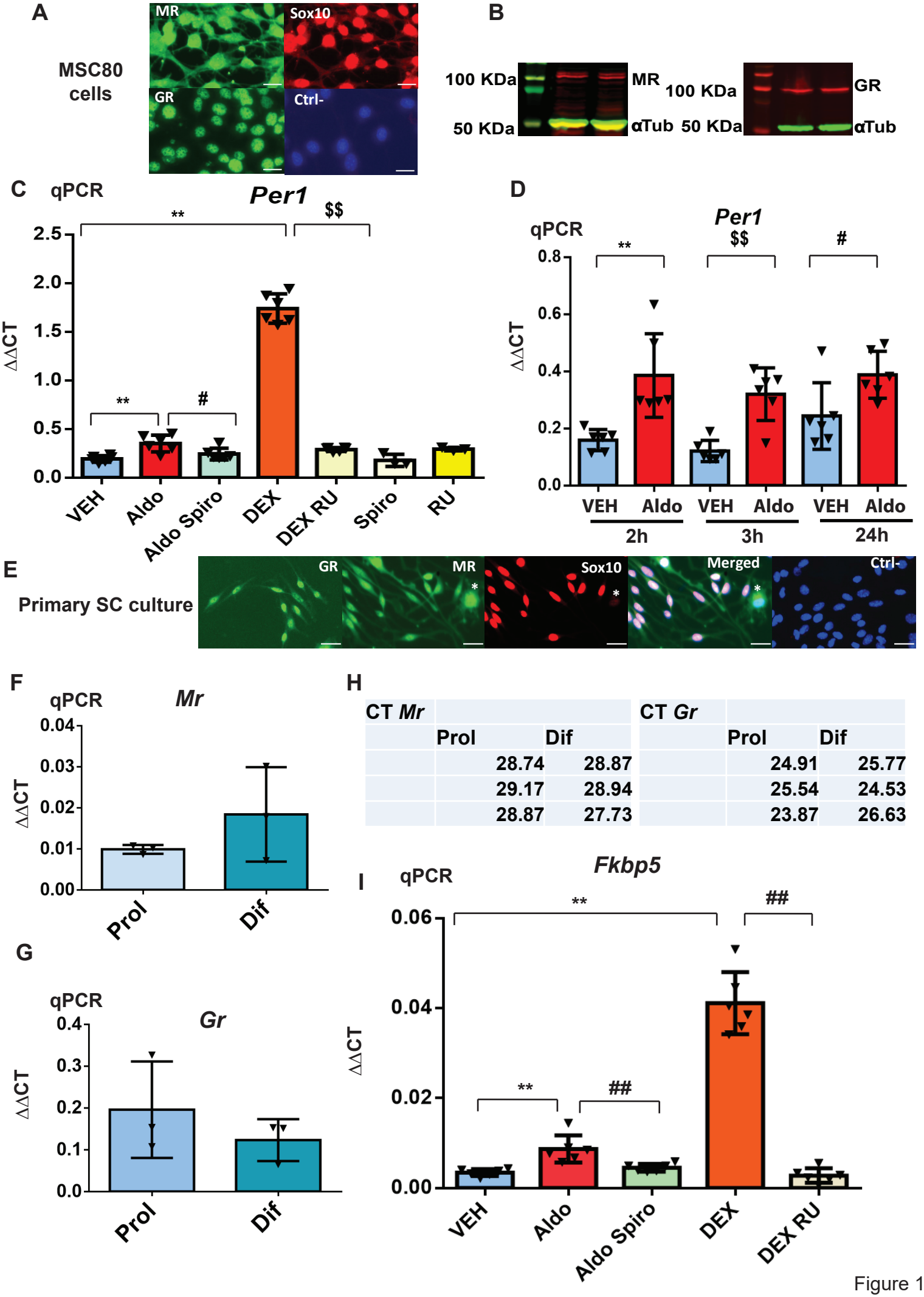
A
MSC80 cells
MR
Sox10
GR
Ctrl-
B
100 KDa
MR
50 KDa
αTub
100 KDa
GR
50 KDa
αTub
C
qPCR
Per1
**
$$
**
#
ΔΔCT
2.5
2.0
1.5
1.0
0.5
0.0
VEH
Aldo
Aldo Spiro
DEX
DEX RU
Spiro
RU
D
qPCR
Per1
**
$$
#
ΔΔCT
0.8
0.6
0.4
0.2
0.0
VEH
Aldo
VEH
Aldo
VEH
Aldo
2h
3h
24h
E
Primary SC culture
GR
MR
Sox10
Merged
Ctrl-
F
qPCR
Mr
ΔΔCT
0.04
0.03
0.02
0.01
0.00
Prol
Dif
H
CT Mr
Prol
Dif
28.74
28.87
29.17
28.94
28.87
27.73
CT Gr
Prol
Dif
24.91
25.77
25.54
24.53
23.87
26.63
G
qPCR
Gr
ΔΔCT
0.4
0.3
0.2
0.1
0.0
Prol
Dif
I
qPCR
Fkbp5
**
##
ΔΔCT
0.06
0.04
0.02
0.00
**
##
VEH
Aldo
Aldo Spiro
DEX
DEX RU

Figure 1

A

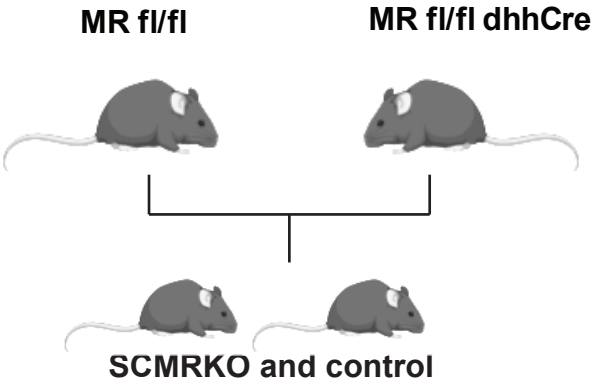

B Genotyping

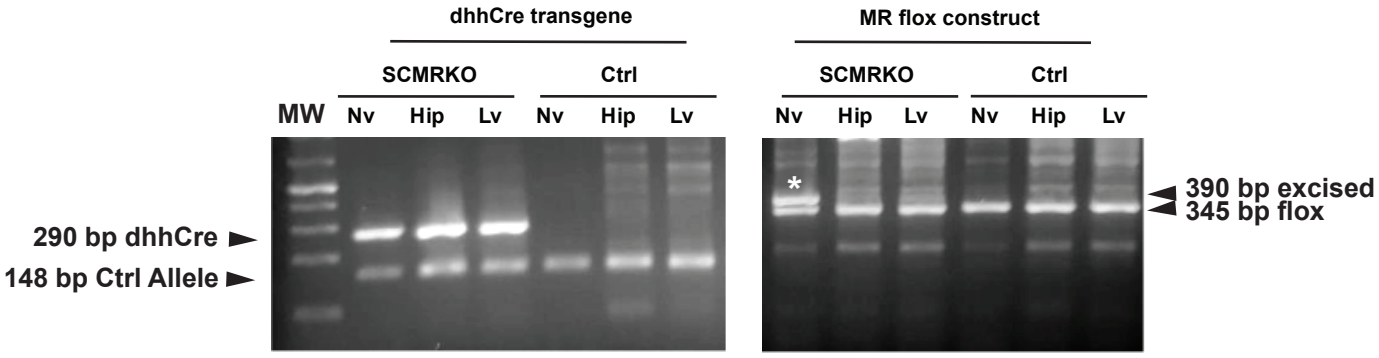

C

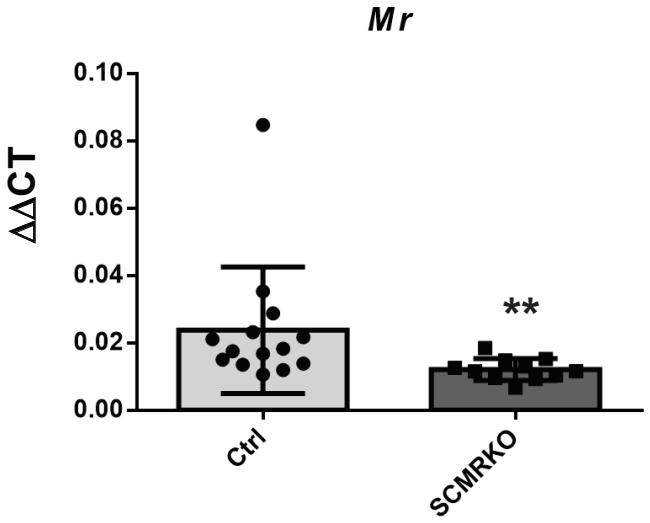

Figure 2

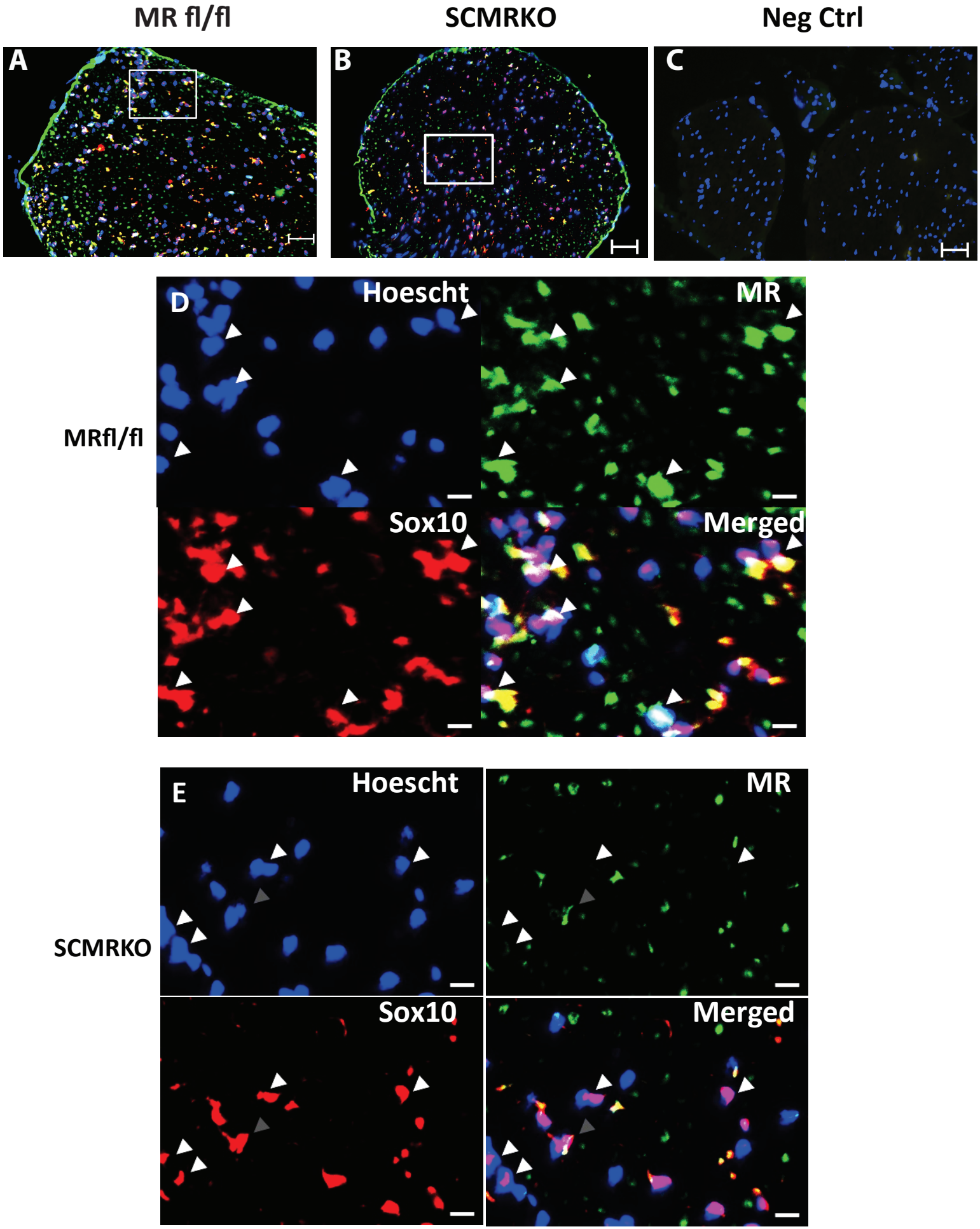
MR fl/fl
SCMRKO
Neg Ctrl
A
B
C
D
Hoescht
MR
MRfl/fl
Sox10
Merged
E
Hoescht
MR
SCMRKO
Sox10
Merged

Figure 3

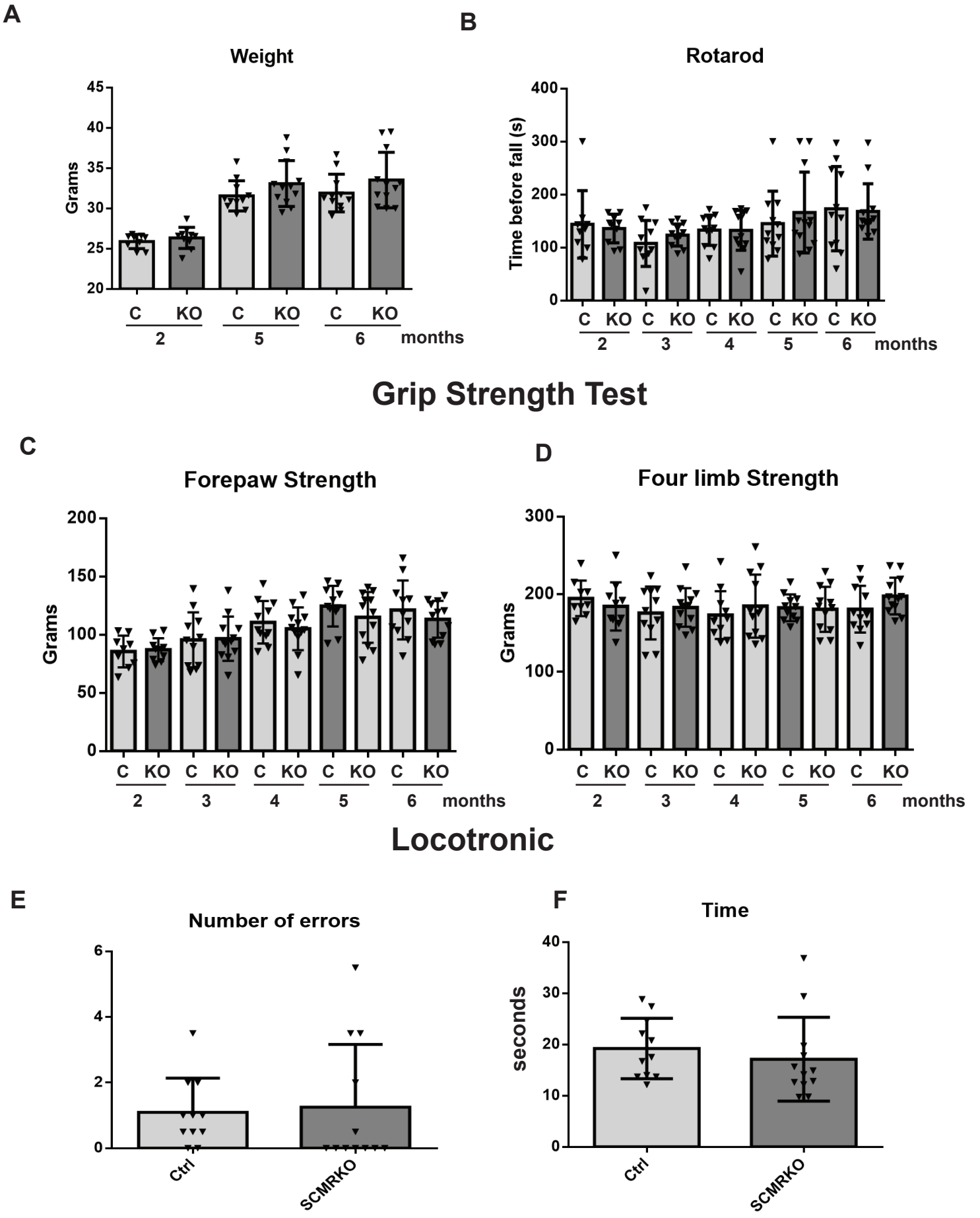
A
Weight
Grams
45
40
35
30
25
20
C KO C KO C KO
2 5 6 months
B
Rotarod
Time before fall (s)
400
300
200
100
0
C KO C KO C KO C KO C KO
2 3 4 5 6 months
Grip Strength Test
C
Forepaw Strength
Grams
200
150
100
50
0
C KO C KO C KO C KO C KO
2 3 4 5 6 months
D
Four limb Strength
Grams
300
200
100
0
C KO C KO C KO C KO C KO
2 3 4 5 6 months
Locotronic
E
Number of errors
6
4
2
0
Ctrl
SCMRKO
F
Time
seconds
40
30
20
10
0
Ctrl
SCMRKO

Figure 4

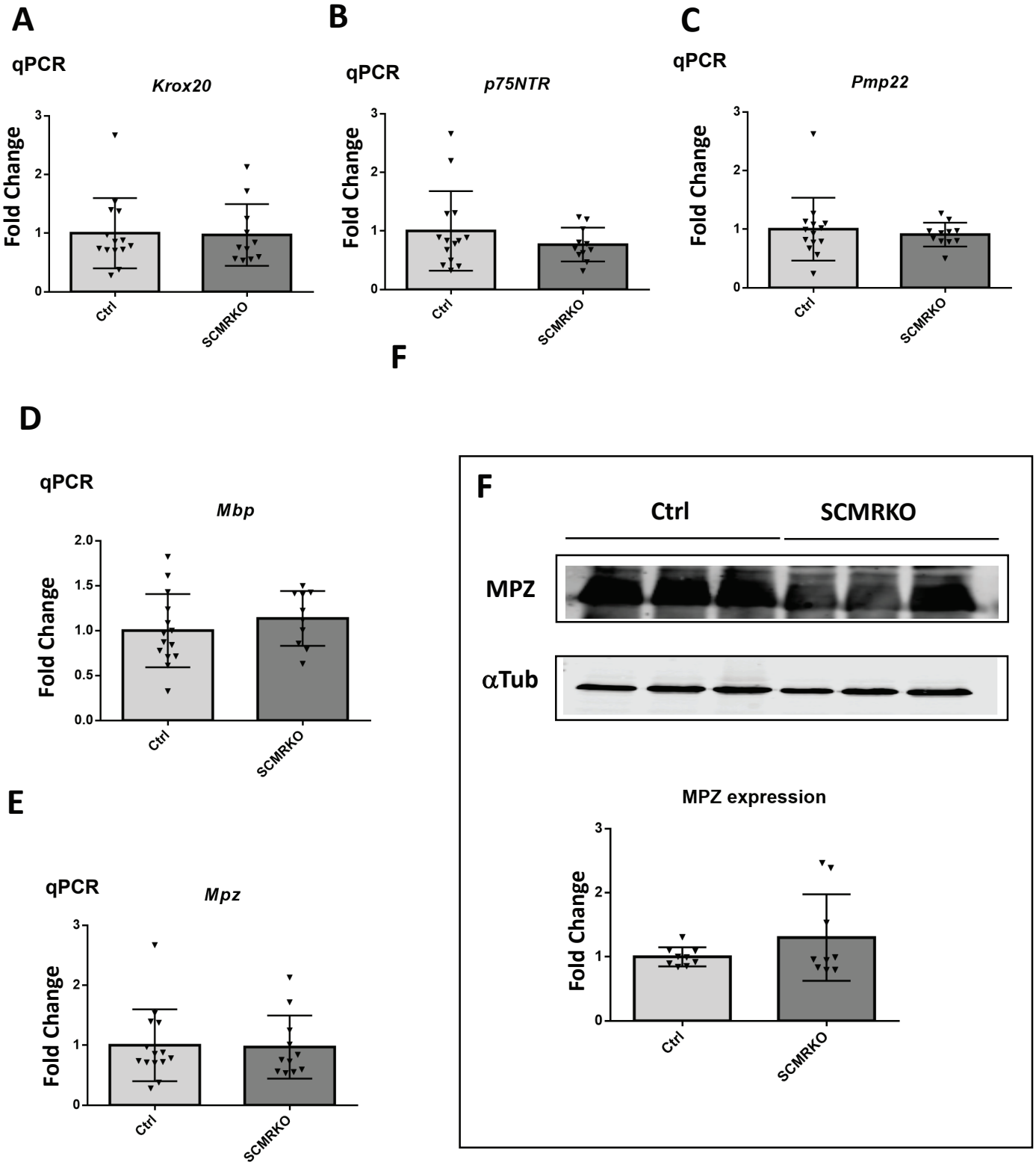
A
qPCR
Krox20
Fold Change
Ctrl
SCMRKO
B
qPCR
p75NTR
Fold Change
Ctrl
SCMRKO
C
qPCR
Pmp22
Fold Change
Ctrl
SCMRKO
D
qPCR
Mbp
Fold Change
Ctrl
SCMRKO
E
qPCR
Mpz
Fold Change
Ctrl
SCMRKO
F
F
Ctrl
SCMRKO
MPZ
αTub
MPZ expression
Fold Change
Ctrl
SCMRKO

Figure 5

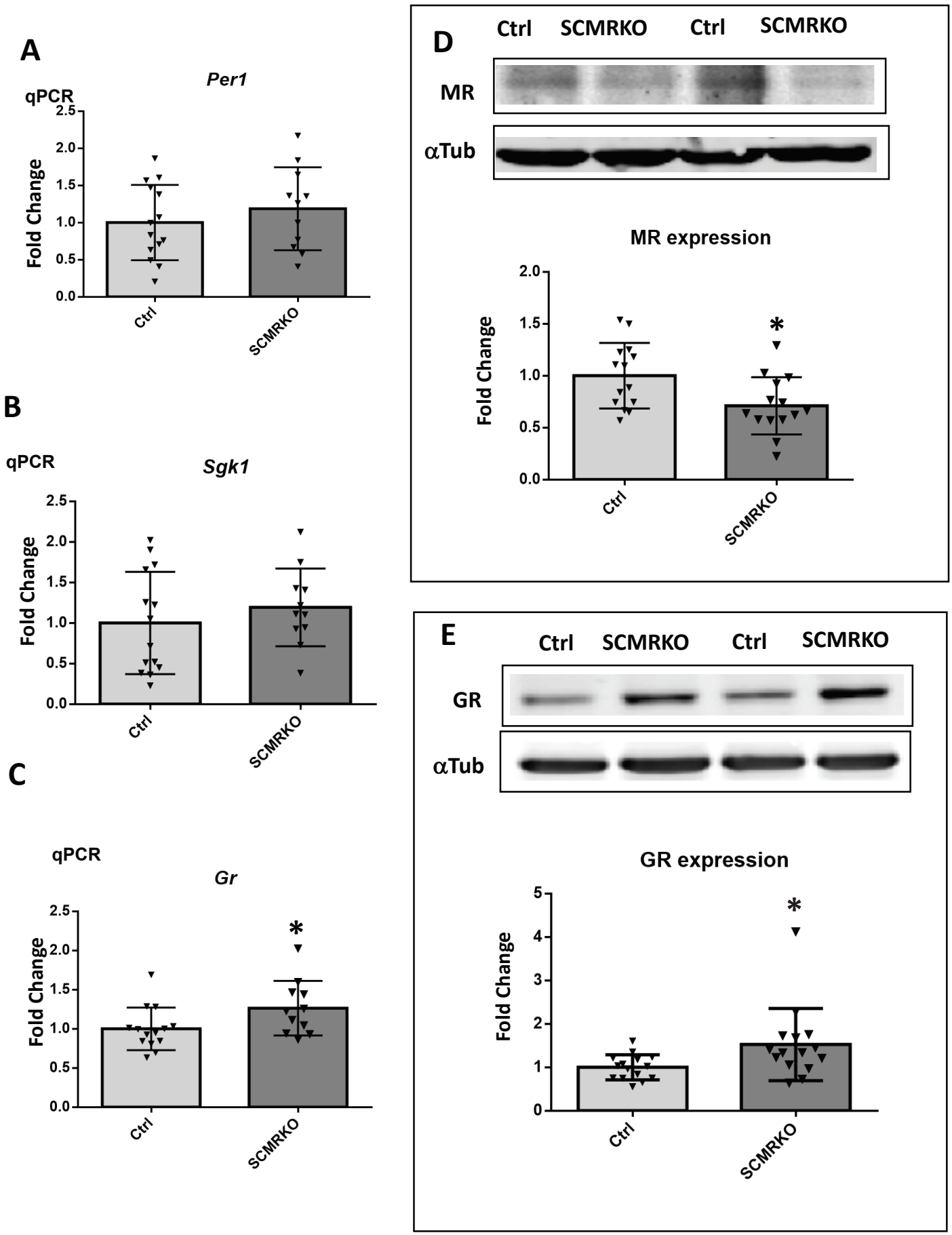
A
Per1
qPCR
Fold Change
2.5
2.0
1.5
1.0
0.5
0.0
Ctrl
SCMRKO
B
qPCR
Sgk1
Fold Change
2.5
2.0
1.5
1.0
0.5
0.0
Ctrl
SCMRKO
C
qPCR
Gr
Fold Change
2.5
2.0
1.5
1.0
0.5
0.0
*
Ctrl
SCMRKO
D
Ctrl
SCMRKO
Ctrl
SCMRKO
MR
αTub
MR expression
Fold Change
2.0
1.5
1.0
0.5
0.0
*
Ctrl
SCMRKO
E
Ctrl
SCMRKO
Ctrl
SCMRKO
GR
αTub
GR expression
Fold Change
5
4
3
2
1
0
*
Ctrl
SCMRKO

Figure 6

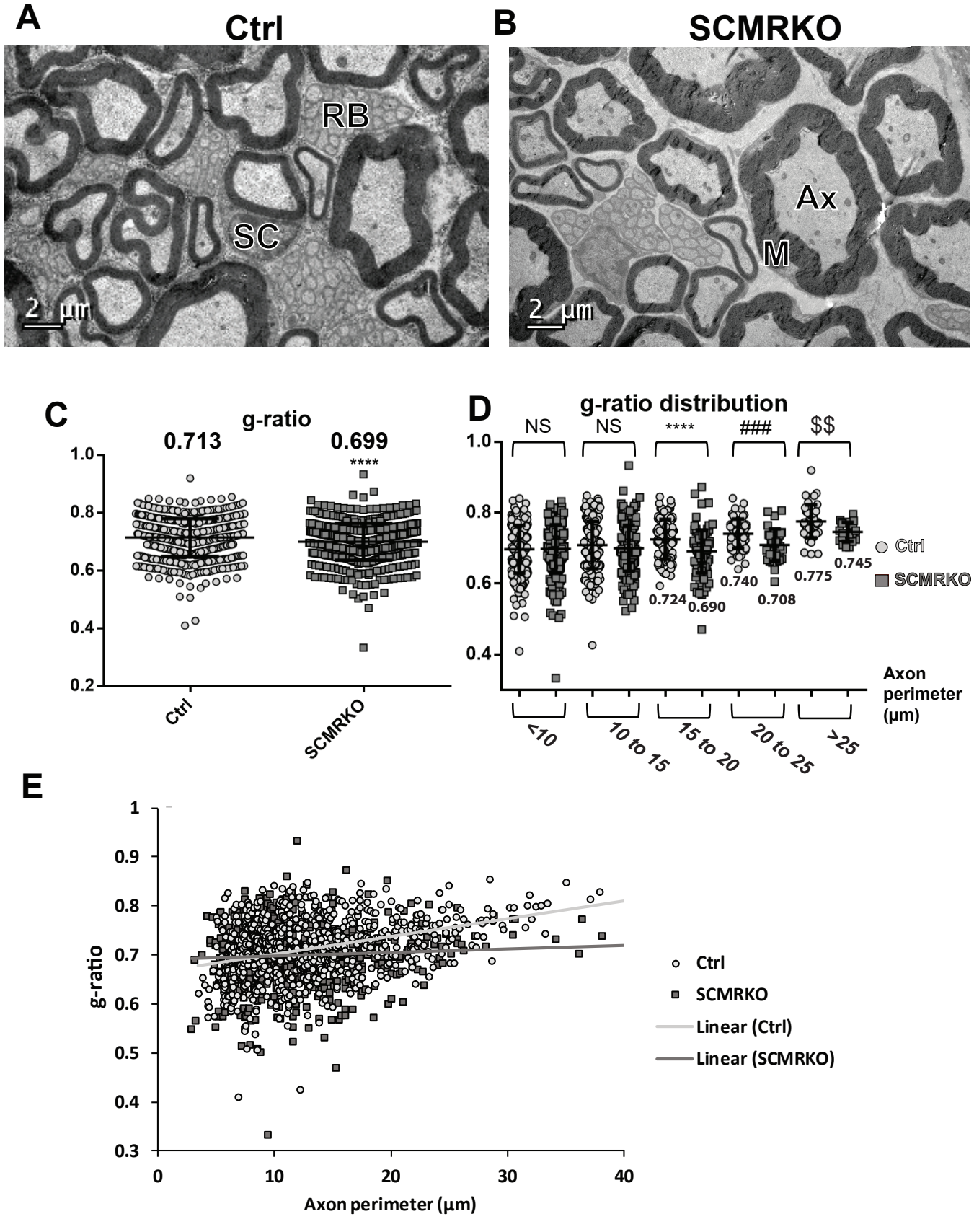
A
Ctrl
RB
SC
2 µm
B
SCMRKO
Ax
M
2 µm
C
g-ratio
0.713
0.699
****
1.0
0.8
0.6
0.4
0.2
Ctrl
SCMRKO
D
g-ratio distribution
NS
NS
****
###
$$
0.724
0.690
0.740
0.708
0.775
0.745
Ctrl
SCMRKO
Axon perimeter (µm)
<10
10 to 15
15 to 20
20 to 25
>25
E
g-ratio
Axon perimeter (µm)
Ctrl
SCMRKO
Linear (Ctrl)
Linear (SCMRKO)

Figure 7

Table 1

Primer name	Sequence (5' to 3')
Genotyping	
dhhCre Fw	AACCTTCTCTAGCGGTGCT
dhhCre Rv	AATCCTTGGCTGAAGGGAAT
D9mit Fw	TAACCAACCCTTGAAGGCAC
D9mit Rv	ACGGACAGCATTTTCCA
MR fl Fw	CTGGAGATCTGAACTCCAGGCT
MR fl Rv1	CCTAGAGTTCCTGAGCTGCTGA
MR fl Rv2	TAGAAACACTTCGTAAAGTAGAGCT
qPCR	
Hsp60 Fw	AGCACGCTGGTTTTGAACAG
Hsp60 Rv	TTCTCCAAACACTGCACCAC
Mrlp10 Fw	AGCTGCGGAAACACAAGATC
Mrlp10 Rv	AAAAGGGGTAGCAGGTTTCG
Rpl13a Fw	TACGCTGTGAAGGCATCAAC
Rpl13a Rv	TTGGTATTCATCCGCTTCCG
Sdha Fw	AGAAAGGCCAAATGCAGCTC
Sdha Rv	GTGAGAACAAGAAGGCATCAGC
Mr Fw	ATGGAAACCACACGGTGACCT
Mr Rv	AGCCTCATCTCCACACACCAAG
Gr Fw	TTCTGTTCATGGCGTGAGTAC
Gr Rv	CCCTTGGCACCTATTCCAGTT
Fkbp5 Fw	AGCTCAGTCCAGCCCATTTC
Fkbp5 Rv	TGTAGAACCCACAGCAGCTG
Sgk Fw	TCACTTCTCATTCCAGACCGC
Sgk Rv	ATAGCCCAGGGCACTGGCTA
Per1 Fw	CCTGGAATTGGAGCATAT
Per1 Rv	CCTGCTCCGAAATATAGACAATC
Krox20 Fw	TGCACCTAGAAACCAGACCTTC
Krox20 Rv	TGCCCGCACTCACAATATTG
Mpz Fw	ATCTCTTTTACCTGGCGCTACC
Mpz Rv	ACTGGATGCGCTCTTTGAAG
Pmp22 Fw	TCTGGCAGAACTGTACCACATC
Pmp22 Rv	TGGCAGAAGAACAGGAACAGA
MBP Fw	ACTCACACACGAGAACTACCC
MBP Rv	GGTGTTCGAGGTGTCACAATG
P75 Fw	AGGTGCCAAGGAGACATGTTC
P75 Rv	CGTCAGAGAACGTAACACTGTC